

# COMPARATIVE STUDY OF BLIND SOURCE SEPARATION METHODS FOR RAMAN SPECTRA

## *Application on Numerical Dewaxing of Cutaneous Biopsies*

Valeriu Vrabie<sup>†</sup>, Cyril Gobinet<sup>‡</sup>, Michel Herbin<sup>†</sup> and Michel Manfait<sup>‡</sup>

<sup>†</sup>*CRESTIC, Université de Reims Champagne-Ardenne, Chaussée du Port, 51000 Châlons-en-Champagne, France*

<sup>‡</sup>*MéDIAN, CNRS UMR 6142, Université de Reims Champagne-Ardenne, 51 rue Cognacq Jay, 51096 Reims, France*

**Keywords:** Raman Spectroscopy, Paraffin-Embedded Cutaneous Biopsies, Blind Source Separation, Independent Component Analysis, Non-negative Matrix Factorization, Maximum Likelihood Positive Source Separation.

**Abstract:** Raman spectroscopy is a powerful tool for the study of molecular composition of biological samples. Digital processing techniques are needed to separate the wealthy but complex information recorded by Raman spectra. Blind source separation methods can be used to efficiently extract the spectra of chemical constituents. We propose in this study to analyze the performances of four blind source separation methods. Two Independent Component Analysis methods using the JADE and FastICA algorithms are based uniquely on the independence of the spectra. The Non-Negative Matrix Factorization takes into account only the positivity of underlying spectra and mixing coefficients. The Maximum Likelihood Positive Source Separation assumes both the independence and positivity of the spectra. A realistic simulated dataset allows a quantitative study of these methods while a real dataset recorded on a paraffin-embedded skin biopsy provides a qualitative study.

## 1 INTRODUCTION

Raman spectroscopy is a light scattering technique used in numerous biomedical applications (Choo-Smith et al., 2002). For example, it was successfully used in oncology to discriminate between malignant and benign tumors (Haka et al., 2002; Gnidecka et al., 2004). Recording the Raman scattering of a laser on a biopsy, the Raman spectroscopy gives information about the vibrational modes of the analyzed sample. Based on the uniqueness of Raman signatures of each molecular constituent, this technique extracts wealthy but complex information about the molecular composition of biopsies.

To be studied in optimal and reproducible conditions by Raman spectroscopy, thin sections of biopsies are required. A conservative property of these biopsies is also needed for their storage in tissue banks (tumor banks in oncology) for further analysis. To satisfy these requirements, the biopsies are fixed by formalin and embedded into paraffin. However, the paraffin has a Raman signature made up of energetic peaks that strongly overlap the signature of the biopsy. Visual analysis of Raman bands (shape, wave-

length localization, etc.) or classical signal processing methods such as Principal Component Analysis (Haka et al., 2002) will be biased for a signature extraction objective. A solution is to chemically dewax and rehydrate the biopsies before analyzing them by Raman spectroscopy. Nevertheless, this process has several drawbacks such as: it is time and reagent consuming, the biopsies are altered and a residual layer of paraffin may remain (Faoláin et al., 2005).

To overcome these problems, an advanced signal processing method based on Independent Component Analysis (ICA) was recently proposed (Vrabie et al., 2007). This method has been shown efficient to model the recorded spectra as a linear mixing of independent Raman spectra, allowing to extract the signatures of the paraffin and, thus, to numerically dewax the biopsies. It also allows to extract the spectrum of the underlying biopsy (human skin) and therefore to define molecular descriptors specific to melanomas and nevi. However, the extraction of Raman spectra is not perfect because some residual paraffin peaks remain on estimated spectra. This might be a consequence of estimated negative peaks, as this method does not take into account the positivity of the spectra and associ-

ated mixing coefficients.

In this paper we propose a comparative study of four methods of blind source separation for numerical dewaxing of paraffin-embedded skin biopsies. The first one employs the Joint Approximate Diagonalization of Eigenmatrices (JADE) algorithm (Cardoso and Souloumiac, 1993). The second one, named FastICA (Hyvärinen et al., 2001), uses a fast fixed-point algorithm. It is employed here in its deflation scheme in which the spectra are estimated one by one. These two methods are ICA-based methods that only assume the independence of the spectra to be estimated. Next, we consider the Non-Negative Matrix Factorization (NMF) which takes into account only the positivity of underlying spectra and mixing coefficients (Lee and Seung, 1999). Finally, the Maximum Likelihood Positive Source Separation (MLPSS) assumes both the independence and positivity of the spectra to be estimated and was developed for the blind separation of Raman spectra (Moussaoui, 2005). A quantitative study is proposed by considering the results given by these methods on a realistic simulated dataset, while a qualitative study is illustrated on a dataset recorded on a paraffin-embedded skin biopsy.

## 2 RAMAN SPECTRA

The Raman spectrum  $\mathbf{R}_k$  is defined as a  $N_V$  dimensional vector made up by the Raman intensities recorded at different wavenumbers into a measurement point  $k$ . By scanning  $K$  points of a sample, the Raman spectroscopy provides a matrix dataset  $\mathbf{R} = [\dots, \mathbf{R}_k, \dots] \in \mathbb{R}^{K \times N_V}$ .

The recorded dataset  $\mathbf{R}$  can be modeled as a linear sum of spectra  $\mathbf{S}_i \in \mathbb{R}^{N_V}$  of chemical constituents, called also sources, weighted by the corresponding mixing coefficients  $\mathbf{A}_i \in \mathbb{R}^K$ , called also concentration profiles (Vrabie et al., 2007):

$$\mathbf{R} = \sum_{i=1}^M \mathbf{A}_i \mathbf{S}_i^T + \mathbf{N}_1 + \mathbf{N}_2. \quad (1)$$

The noise  $\mathbf{N}_1$  describes a part of the noise that is made up by sources related to useless chemical constituents that might be present in acquisition or by a linear additive recorded noise. The noise  $\mathbf{N}_2$  denotes a non-linear additive noise (i.e. not having a linear behavior from a spectrum to another) made up principally by slow-varying parasitic fluorescence. Since they are generated by unrelated phenomena, the noise  $\mathbf{N}_1$  is supposed decorrelated from the interesting spectra  $\mathbf{S}_i$ . Note that the spectra of the chemical constituents and the mixing coefficients admit only positive values by definition.

This model does not take into account the deforming effects that might appear in real acquisitions such as the spectral shifts or width variations of the Raman peaks. These deforming effects and the noise  $\mathbf{N}_2$  can be removed from the recorded spectra by preprocessing techniques (Gobinet et al., 2007). We note thereafter with  $\mathbf{R}_{sig} = \mathbf{R} - \mathbf{N}_2$  the subspace of dimension  $P$  obtained after the preprocessing, which is made up by the interesting spectra and the linear noise  $\mathbf{N}_1$ .

For paraffin-embedded biopsies, the value of  $M$  can be usually fixed at 5 for cases where the Raman signature of the fixation slide (as for example CaF<sub>2</sub> slide) is owing to the recorded spectral range or at 4 otherwise. Moreover, it was proved that the paraffin is completely described by three sources  $\mathbf{S}_1, \mathbf{S}_2, \mathbf{S}_3$  having non-overlapping thin peaks (Vrabie et al., 2007). These sources being modeled as sparse and non-Gaussian, all higher-order cross cumulants of the  $M$  sources considered in (1) vanish, assuring the independence of these sources.

Retrieving the spectra of the chemical constituents can be thus formulated as a source separation problem based on the assumption that these sources are positive and independent.

## 3 BSS METHODS

Blind source separation (BSS) consists in recovering unobserved sources  $\mathbf{S}_i$  from several observed mixtures  $\mathbf{R}$  with no a priori information about the mixing coefficients  $\mathbf{A}_i$ . The lack of a priori knowledge about the mixture is compensated by physically plausible assumption on the sources such as decorrelation, independence and/or positivity. A review of the BSS approaches can be found in (Cardoso, 1998).

BSS methods usually suppose that the number of sources is smaller than the number of observed mixtures and that the dataset is noise-free. Generally, the number of recorded spectra (i.e.  $K$  in our case) being at least one hundred spectra, the first assumption holds. The second one is not respected by the subspace  $\mathbf{R}_{sig}$  since the noise  $\mathbf{N}_1$  remains after the preprocessing. Based on the assumption that this noise is decorrelated from the interesting spectra, it can be estimated and removed by decomposing the subspace  $\mathbf{R}_{sig}$  in two orthogonal subspaces by the use of the Singular Value Decomposition (Vrabie et al., 2007):

$$\mathbf{R}_{sig} = \sum_{j=1}^M \delta_j \mathbf{U}_j \tilde{\mathbf{S}}_j^T + \sum_{j=M+1}^P \delta_j \mathbf{U}_j \tilde{\mathbf{S}}_j^T, \quad (2)$$

Note that this decomposition can be linked with the well known Principal Component Analysis (PCA). The second subspace is an estimate of the noise

$\mathbf{N}_1$ . The first subspace is constructed by decorrelated spectra  $\tilde{\mathbf{S}}_j$ , which are still a linear mixing of interesting spectra, and fit the BSS model. The spectra of paraffin being modeled by independent sources, stronger criteria than decorrelation must be used to extract them. Note that this decomposition may introduce negative values in the first subspace, especially when the recorded intensities are weak, which is not usually the case in Raman spectroscopy. In these cases, the above subspace reduction can be replaced by a random projection of the dataset  $\mathbf{R}_{sig}$  into a positive matrix having  $M$  lines (Moussaoui, 2005).

### 3.1 ICA

The Independent Component Analysis (ICA) is a computational technique for the BSS problem based on the only assumption that the sources are mutually independent and at most one is Gaussian. A detailed description can be found in (Hyvärinen et al., 2001). We focus here only on two ICA algorithms: JADE (Cardoso and Souloumiac, 1993) and FastICA (Hyvärinen et al., 2001).

ICA has two indeterminacies: the energies (variances) and the order of the independent components (estimated spectra) cannot be determined. The first ambiguity is avoided by estimating independent components of unit variances. This is not a restriction for this kind of application since we are interested to identify the spectrum of the biopsy in order to find molecular descriptors. Moreover, the ambiguity of the sign of the estimated spectra is not avoided, but this is insignificant since the sign can be found in the mixing coefficients. For these reasons and to simplify the theory and the algorithms, the dataset  $\mathbf{R}_{sig}$  is centered by subtracting the mean of each spectrum. Each observation is also normalized to unit variance, ensuring that even weak-amplitude recorded observations are well represented within the input data.

#### 3.1.1 JADE Algorithm

The 4<sup>th</sup> order cross-cumulants of the decorrelated sources  $\tilde{\mathbf{S}}_j$  given by PCA in Eq. (2) are firstly computed. A  $M \times M \times M \times M$  dimensional tensor is obtained, which must be diagonalized in order to find independent sources. The Joint Approximate Diagonalization of Eigenmatrices (JADE) algorithm (Cardoso and Souloumiac, 1993) uses the joint diagonalization of cumulant matrices obtained by unfolding the obtained 4<sup>th</sup> order tensor. This step provides a  $M \times M$  rotation matrix  $\mathbf{B}$  that is used to find independent sources  $\hat{\mathbf{S}}_i$  by multiplying the matrix made up by the decorrelated sources  $\tilde{\mathbf{S}}_j$  with this matrix  $\mathbf{B}$ . The

$\hat{\mathbf{S}}_i$ 's are centered and normalized estimators of the interesting spectra  $\mathbf{S}_i$ .

#### 3.1.2 FastICA

The FastICA algorithm is based on a fixed-point iteration scheme for finding directions in which the negentropy is maximized. Beyond the very fast convergence of this algorithm (at least quadratic), the algorithm finds directly independent components of (practically) any non-Gaussian distribution using a nonlinearity  $g$ , so no estimate of the probability distribution function has to be first available. The nonlinearity can optimize the performance of the method allowing to obtain algorithms that are robust and/or of minimum variance. Moreover, the independent components can be estimated one by one, which is equivalent to a projection pursuit. A detailed description of this algorithm can be found in (Hyvärinen et al., 2001).

This algorithm was employed here in its deflation scheme. The algorithm iteratively finds directions in which the estimated independent components are maximally nongaussian. This technique is appropriate to initially estimate the spectra of the paraffin  $\mathbf{S}_1, \mathbf{S}_2, \mathbf{S}_3$ . The spectrum of the biopsy is hence obtained by deflation as the remaining source.

### 3.2 NMF

Broadly speaking, the Non-Negative Matrix Factorization (NMF) factorizes a matrix made up of non-negative values in two other matrices composed of non-negative values, which multiplied will approximately equalize the original result (Lee and Seung, 1999). The factorization algorithms are based on iterative updates which minimize a criterion such as the least squares error or generalized Kullback-Leibler divergence. These algorithms can only be guaranteed to find local minima, rather than a global minimum, and the obtained results depend on the initialization.

The NMF using a least squares error algorithm was used here in order to test if it is possible to find positive spectra  $\mathbf{S}_i$  and mixing coefficients  $\mathbf{A}_i$  from the dataset  $\mathbf{R}_{sig}$  without further a priori information.

### 3.3 MLPSS

The Maximum Likelihood Positive Source Separation (MLPSS) assumes both the independence and positivity of the spectra to be estimated and has been developed especially for the blind separation of Raman spectra (Moussaoui, 2005). It models the positive independent spectra to be estimated by gamma probability density functions (pdf) with an  $\alpha$  parameter

greater than one. This model is well adapted to spectra of the paraffin  $S_1, S_2, S_3$ .

To solve this problem, two algorithms were proposed. The first one is based on the maximization of the likelihood by using a Monte-Carlo Expectation-Maximization scheme, while the second one combines the above assumptions and the maximum likelihood technique to derive a steepest gradient algorithm. This last algorithm was used here because it is faster and it is well adapted for cases where the noise is small, which is the case of large acquisitions after the noise removal by PCA.

### 3.4 Application

A quantitative study on a realistic simulated dataset is firstly presented followed by a qualitative study on a dataset recorded on a paraffin-embedded skin biopsy.

#### 3.4.1 Simulated Dataset

We consider here four spectra  $S_1, \dots, S_4 \in \mathbb{R}^{990}$  represented in Figure 1. The first three were constructed from a recording on a paraffin block. The peaks were selected by the use of a Hanning window accordingly with the fact that the paraffin is defined by three spectra (Vrabie et al., 2007). The last one is the spectrum of the human skin estimated on a real dataset by an ICA-based BSS method. Note however that linear interpolations were used to eliminate the imperfections corresponding to contributions of paraffin peaks.

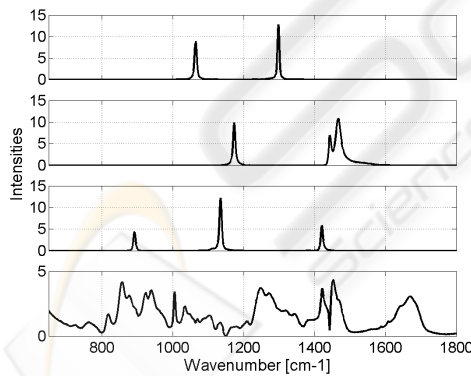


Figure 1: Simulated spectra.

These spectra were linearly mixed to construct  $K = 250$  observations by randomly picking positive mixing coefficients from a mixing matrix obtained on a real dataset. Figure 2 shows one observation. The mixing coefficients of  $S_4$  are very low compared to the others, due to the energetic Raman signatures of the paraffin that are present in real acquisitions. Note that this dataset is free of noise, so the decomposition given in Eq. (2) was not performed here.

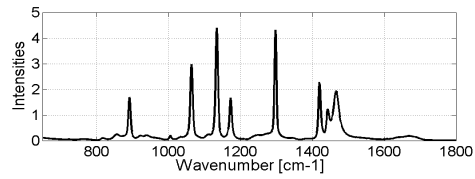


Figure 2: Example of one observation.

The number of sources to be estimated was set at  $M = 4$  for all BSS methods. The dataset was centered and each observation normalized to unit variance before applying the ICA-based methods. A "pow3" nonlinearity  $g$  was chosen for the FastICA because it gives the best estimator for the last spectrum.

The threshold of the least squares error algorithm for NMF was set at  $10^{-10}$ . As the convergence was very slow, a second stop condition was used: the variations of the least squares error from one iteration to other must be smaller than  $10^{-5}$ . Even in this case the convergence was very slow, the number of iterations, which depends on the initialization, was about  $6 \cdot 10^5$ . Note that the results presented here are the best obtained for 20 different initializations of the NMF.

The gradient step size of the MLPSS method was set at  $10^{-3}$ , which is a usual value for this kind of data. The MLPSS method has a faster convergence than NMF, around  $10^4$  iterations are necessary to obtain a good estimate of the spectra. However, the MLPSS did not have a convergence toward a stationary point, so it was stopped after  $5 \cdot 10^5$  iterations.

Figure 3 shows the estimated spectra  $\hat{S}_4$  of the last spectrum  $S_4$  by the presented BSS methods. We focus here only on this spectrum because it corresponds to the underlying biopsy in real applications and its estimation is of interest.

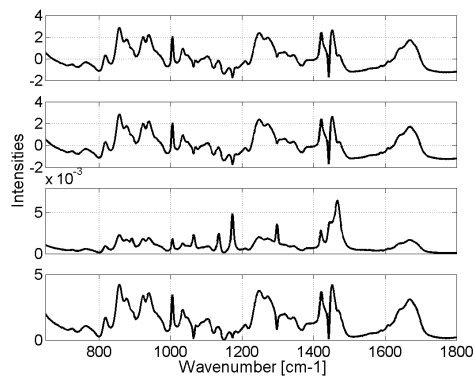


Figure 3: Estimators of the 4<sup>th</sup> spectrum. From top to bottom: JADE, FastICA, NMF and MLPSS.

As we can see, the NMF fails to estimate this spectrum. This is due to the fact that NMF requires the existence of a monomial submatrix in the dataset in order to ensure the convergence of the algorithm to the right solution (Moussaoui, 2005). The MLPSS



provides a good positive estimate with few imperfections corresponding to contributions of paraffin peaks at  $1065 \text{ cm}^{-1}$  and  $1300 \text{ cm}^{-1}$ . The two ICA-based methods give the same results. The estimated spectra have zero mean and unit variance and follow the shape of the original spectrum except some imperfections at  $1175 \text{ cm}^{-1}$  and  $1470 \text{ cm}^{-1}$ . Note that all estimated mixing coefficients have uniquely positive values, even for the ICA-based methods.

In order to provide a quantitative study we compute the root mean square error (RMSE):

$$\text{RMSE} = \left\| \bar{\mathbf{S}}_4 - \hat{\mathbf{S}}_4 \right\| / \sqrt{N_T} \quad (3)$$

where  $\|\cdot\|$  denotes the Frobenius norm and  $\bar{\mathbf{S}}_4$  the centered and normalized version of the original spectrum  $\mathbf{S}_4$  used to construct the mixtures.  $\hat{\mathbf{S}}_4$  denotes either the spectra estimated by ICA-based methods or the centered and normalized versions of the spectra estimated by NMF or MLPSS.

The values of RMSEs obtained for the estimated spectra (see figure 3) are: 0.1605 for JADE, 0.1603 for FastICA, 0.8017 for NMF and 0.1264 for the MLPSS algorithm. These values confirm that ICA-based methods give practically the same results and that NMF fails to estimate this spectrum. Moreover, we can conclude that the MLPSS method gives the best estimate, which, additionally, has positive values.

In the following we consider the case where a linear noise  $\mathbf{N}_1$ , decorrelated from the interesting spectra, is added to the observations. We have chosen here a Gaussian noise for the sake of simplicity. This noise also simulates slight deforming effects on the peaks of paraffin that may remain after the preprocessing steps in real cases. This study is done by varying the signal-to-noise ratio (SNR):

$$\text{SNR} = 20 \log_{10} \frac{\left\| \sum_{i=1}^4 \mathbf{A}_i \mathbf{S}_i^T \right\|}{\left\| \mathbf{N}_1 \right\|} \quad [dB] \quad (4)$$

Note that the decomposition (2) does not completely remove the noise  $\mathbf{N}_1$ . After this step, a gain of  $17dB$  is obtained for high values of SNR (i.e.  $\text{SNR} = 50dB$ ). This gain linearly decreases with the SNR, a gain of  $6.5dB$  being obtained for a  $\text{SNR} = 2.5dB$ .

Figure 4 shows the evolutions of the RMSEs for the estimated spectrum  $\hat{\mathbf{S}}_4$  with respect to the SNR. These values are averaged over 4 independent realizations of the noise. The values obtained by the JADE algorithm (represented by “■”) are superposed on those obtained for the FastICA (represented by “×”). These evolutions confirm the conclusion stated above even if, punctually, the RMSE of the MLPSS is larger than the ones obtained by ICA methods.

Although these results give the MLPSS as the best separation method, it is interesting to study the errors

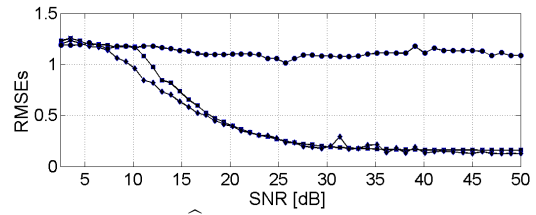


Figure 4: RMSEs of  $\hat{\mathbf{S}}_4$  with respect to the SNR: “■” JADE, “×” FastICA, “•” NMF, “◆” MLPSS.

of, for example, the estimator  $\hat{\mathbf{S}}_3$  of the third spectrum of the paraffin. These errors are shown in Figure 5.

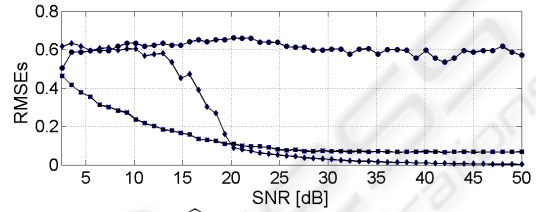


Figure 5: RMSEs of  $\hat{\mathbf{S}}_3$  with respect to the SNR: “■” JADE, “×” FastICA, “•” NMF, “◆” MLPSS.

The result obtained for the MLPSS method is due to the fact that the same peak of the paraffin is extracted by two estimators,  $\hat{\mathbf{S}}_2$  and  $\hat{\mathbf{S}}_3$ . For real applications this effect can perturb the estimator of the biopsy, especially when the preprocessing does not completely compensate the deforming effects.

### 3.4.2 Real Dataset

The study is done on a dataset composed of  $K = 1254$  Raman spectra acquired on a paraffin-embedded skin biopsy. Spectral data were recorded into  $N_T = 990$  points in the  $650-1816 \text{ cm}^{-1}$  range by using a Labram microspectrometer. The preprocessing techniques developed in (Gobinet et al., 2007) are firstly used in order to improve the estimated spectra.

Figures 6, 7 and 8 show the results obtained by the JADE, NMF and MLPSS algorithms. The results of the FastICA being the same with those given by JADE are not presented here. The same parameters as in the simulated case were used. Some residual peaks of paraffin, which sometimes are negative, are present on spectra estimated by the JADE algorithm. However, this technique provides positive mixing coefficients. The spectrum of the biopsy estimated by NMF contains more energetic residual peaks of the paraffin than the JADE estimator, whereas the spectra of the paraffin are not well estimated. Spectra estimated by MLPSS are close to the JADE results, but the same peak of the paraffin ( $1135 \text{ cm}^{-1}$ ) is extracted by two estimators as in the simulated case. Moreover, the application of this algorithm on another paraffin-embedded skin biopsy led to a wrong estimation of spectra, contrary to JADE.

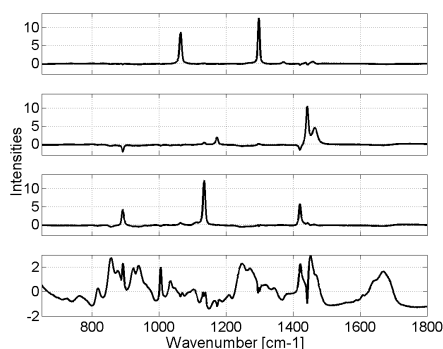


Figure 6: Spectra estimated by JADE.

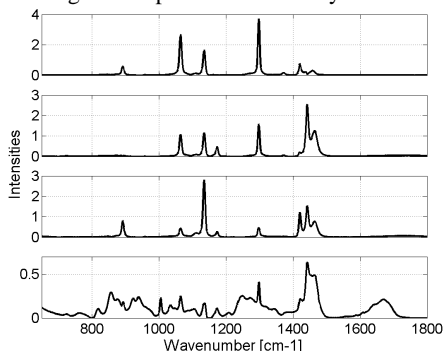


Figure 7: Spectra estimated by NMF.

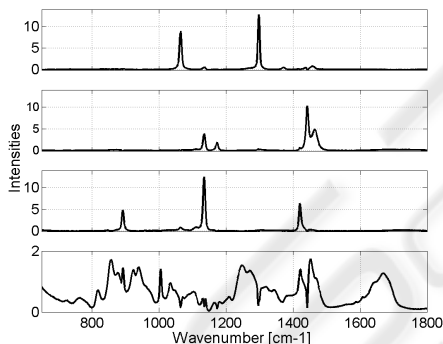


Figure 8: Spectra estimated by MLPSS.

## 4 CONCLUSIONS

Four BSS methods were studied on simulated and real datasets. Taking into account only the positivity, the NMF fails to estimate the interesting spectra. The positivity combined with the independence allows the MLPSS method to provide a good estimator for the biopsy, but artefacts are obtained for the paraffin for which the same peak is extracted by more than one estimator. Furthermore, the results obtained by this method depend on the analyzed biopsy. ICA-based methods give good estimators for all spectra, which do not depend on the biopsies, and extract positive mixing coefficients. These last methods can thus be employed as an efficient tool for the extraction of Ra-

man spectra of chemical species and consequently for a numerical dewaxing of biopsies. However, all these methods allow to extract a unique spectrum of the skin, which might be insufficient for a classification purpose. Investigations are under way for the study of a numerical dewaxing based on least square methods, taking into account the Raman spectra of the paraffin estimated on paraffin blocks.

## REFERENCES

- Cardoso, J.-F. (1998). Blind signal separation: statistical principles. *Proceedings of the IEEE*, 86:2009–2025.
- Cardoso, J.-F. and Souloumiac, A. (1993). Blind beam-forming for non-gaussian signals. *IEE Proceedings-F*, 140:362–370.
- Choo-Smith, L.-P., Edwards, H., Endtz, H., Kros, J., Heule, P., Barr, H., Robinson, J., Bruining, H., and Puppels, G. (2002). Medical applications of Raman spectroscopy: from proof of principle to clinical implementation. *Biopolymers*, 67:1–9.
- Faoláin, E., Hunter, M., Byrne, J., Kelehan, P., Lambkin, H., Byrne, H., and Lyng, F. (2005). Raman spectroscopic evaluation of efficacy of current paraffin wax section dewaxing agents. *Journal of Histochemistry and Cytochemistry*, 53:121–129.
- Gniadecka, M., Philipsen, P., Sigurdsson, S., Wessel, S., Nielsen, O., Christensen, D., Hercogova, J., Rossen, K., Thomsen, H., Gniadecki, R., Hansen, L., and Wulf, H. (2004). Melanoma diagnosis by Raman spectroscopy and neural networks: Structure alterations in proteins and lipids in intact cancer tissue. *The Journal of Investigative Dermatology*, 122:443–449.
- Gobinet, C., Vrabie, V., Tfayli, A., Piot, O., Huez, R., and Manfait, M. (2007). Pre-processing and source separation methods for Raman spectra analysis of biomedical samples. In *Proceedings of the 29th Annual International Conference of the IEEE Engineering in Medicine and Biology Society, Lyon, France*.
- Haka, A., Shafer-Peltier, K., Fitzmaurice, M., Crowe, J., Dasari, R., and Feld, M. (2002). Identifying microcalcifications in benign and malignant breast lesions by probing differences in their chemical composition using Raman spectroscopy. *Cancer Research*, 62:5375–5380.
- Hyvärinen, A., Karhunen, J., and Oja, E. (2001). *Independent Component Analysis*. Wiley, New York.
- Lee, D. and Seung, H. (1999). Learning the parts of objects by non-negative matrix factorization. *Nature*, 401:788–791.
- Moussaoui, S. (2005). *Séparation de sources non-négatives. Application au traitement des signaux de spectroscopie*. PhD thesis, CRAN INPL, Nancy, France.
- Vrabie, V., Gobinet, C., Piot, O., Tfayli, A., Bernard, P., Huez, R., and Manfait, M. (2007). Independent component analysis of Raman spectra: Application on paraffin-embedded skin biopsies. *Biomedical Signal Processing and Control*, 2:40–50.